

# Synthesis, Characterizations and Properties of Wide Band Gap Semiconductors and Ferrite Nanoparticles

Sangeeta Bakshi and Mohit Sahni\*

Department of Physics and Environmental Sciences, Sharda School of Engineering and Science, Sharda University, Greater Noida, Uttar Pradesh, India

\*Corresponding Author: mohit.sahni@sharda.ac.in

**Abstract:** In this manuscript detailed review was done on the synthesis, characterization and properties of two widely used materials, one is wide band gap semiconductors and second is ferrite nanoparticles for photocatalytic activities and dye degradation. The water pollution due to toxic dyes used in most of the textile industries is a big issue which need to be addressed and this manuscript deals with the solution to the problem. The synthesis of nanoparticles of individual material and their composite is explained in the manuscript. The modification in the properties of the composite is also explained.

**Keywords:** Ferrite, Magnetic, Nanoparticles, Photocatalytic, Wide band gap.

## I. INTRODUCTION

The growing need for smaller technology devices has led to an increase in the significance of nanoscale magnetic materials. Improving the performance of permanent magnetic materials requires an understanding of magnetic characteristics at the nanoscale. The magnetic characteristics of nanoparticles are greatly influenced by their size, shape, surface effects, magnetic anisotropy, and other factors (Salih and Mahmood, 2023).

Growing volumes of wastewater from industrial, agricultural, and other human activities have damaged the environment over time, bringing with them harmful organic and inorganic contaminants and toxic heavy metals and human activities have polluted the global aquatic ecosystem. Water pollution is mostly caused by the textile industry (Brillas and Garcia-Segura, 2023). Textile wastewaters contain a range of non-biodegradable organic dyes as Rhodamine B, Congo red (CR) secondary diazo dye and methylene blue (MB) and other contaminants at different quantities that are harmful to ecosystem health, mutagenic, carcinogenic, and non-recyclable (Hosny *et al.*, 2023; Salih and Mahmood, 2023). Coloured effluents from dyeing companies not only contaminate water but also impede photosynthesis and autotrophic creature activity, resulting in a decrease in oxygen production and an imbalance in the surrounding environment (Oliveira *et al.*, 2022).

Eliminating these pollutants from the water is essential to reducing the growing global water crisis (Gupta *et al.*, 2020). Many methods, such as ion exchange, exchange adsorption, ozonation, electrolysis, electrodialysis, membrane filtration, coagulation, chemical precipitation, flocculation, Fenton reaction, reductive degradation, microbial processes, and photocatalytic degradation, reverse osmosis, electrostatic precipitation, adsorption, chemical precipitation are used to remove dyes from industrial waste water (Luque-Morales *et al.*, 2021). Due to their high operating costs, sludge creation, or secondary pollution formation, these techniques are not widely used in practice (Tamboli *et al.*, 2023). Photocatalysis is a simple, inexpensive method that breaks down organic dye pollution into nontoxic compounds by using solar light or UV radiation. It also doesn't produce any harmful byproducts (Taymaz *et al.*, 2023). It converts organic dyes, either fully or partially, into non-toxic byproducts. (Gupta *et al.*, 2020).

Small particle size, big specific surface area, and high surface energy nanomaterials have been explored as potential photocatalysts to offer new solutions to waste water treatment (Sun *et al.*, 2023). As semiconductors, photocatalysts are highly efficient at degrading organic pollutants because of their high degradation efficiency, reusability, ease of handling, and low concentration requirements. Today, oxide semiconductor nanoparticles (NPs) such as titanium dioxide (TiO<sub>2</sub>), tin dioxide (SnO<sub>2</sub>), copper oxide (CuO), iron oxide (III) (Fe<sub>2</sub>O<sub>3</sub>), wolfram oxide (WO<sub>3</sub>), ZnO, or their mixtures are the most commonly utilized as photocatalysts. TiO<sub>2</sub> and ZnO nanoparticles (NPs), two semiconducting metal oxides, hve drawn a lot of attention because of their strong photocatalytic activity, broad band gaps of 3.4 eV and 3.37 eV, good chemical and thermal stability, low toxicity, eco-friendliness, etc. High levels of ionic bonding are also present in metal oxide nanoparticles. Modifications to the photocatalyst's structure through doping or the creation of a composite to alter its surface increases the activity of the photocatalyst further (Kanwal *et al.*, 2023; Rajan *et al.*, 2023).

Zinc oxide (ZnO) is one of the most widely utilised nanoparticles in various applications such as gas sensors, paint, adsorption, rubber additives, and superconductors,

luminous material, sensors, solar cells, batteries, optoelectronic applications, etc. (Rajan *et al.*, 2023). It is regarded as one of the best photocatalysts for the breakdown of pollutants in water due to their favourable band-gap of around 3.37 eV and shown photosensitivity. As an n-type, ZnO transistor using a Wurtzite configuration (Luque-Morales *et al.*, 2021).

Few substances possess the dual capabilities of photo-oxidation and photo-reduction, which enables them to efficiently eliminate dangerous chemical molecules in visible light. Because of their bandgap that can absorb visible light and spinel crystal structure, ferrites are great candidates for photocatalysis. They have the ability to break down a variety of pollutants. Because of its high electrical resistance, low eddy current losses, and magnetic characteristics, magnetic spinel ferrite materials are a family of ferrimagnetic ceramics that find application in a range of electric and optoelectronic devices (Salih and Mahmood, 2023).

The removal of pollutants from wastewaters is greatly aided by magnetic nanoparticles, particularly iron magnetic nanoparticles, due to their high surface area per volume, high high disposability, capacitance in adsorption, low toxicity, low mass transfer limitation and ease of separation when compared to other catalysts. Spinel ferrites have the typical chemical formula  $AB_2O_4$ , where B is iron (III) oxide in the  $+3$ -oxidation state ( $Fe_2O_3$ ) and A is a metal ion, such as Co, Cu, Zn, Mg, Ni, Fe, Cd, or another metal. These materials efficiently absorb light in the visible spectrum because of their tiny band gaps. Depending on their original crystal lattice, ferrites have different structural properties from garnet, hexagonal, and spinel. A single unit cell has 64 tetrahedral and 32 octahedral sites; however, only 8 and 24 sites are occupied by cations in that order. Three forms of spinel—normal, inverse, and mixed—are identified based on the distribution of cations in the octahedral and tetrahedral sites. Ferrites' physicochemical characteristics are greatly influenced by the kinds, amounts, and locations of the metal cations inside the crystalline structure (Salih and Mahmood, 2023).

Spinel ferrites like Magnetic  $CoFe_2O_4$ ,  $MnFe_2O_4$ ,  $CuFe_2O_4$ ,  $ZnFe_2O_4$ , and  $NiFe_2O_4$  have drawn a lot of attention because of their distinctive structural, magnetic, optical, electrical, and dielectric properties as well as their thermal and chemical stability. These properties have also led to a wide range of technological applications, such as photoluminescence, biosensors, humidity sensors, catalysis, magnetic refrigeration, permanent magnets, magnetic drug delivery, and magnetic (hyperthermia) (Salih and Mahmood, 2023). These ferrites with spinel can be connected to Photocatalysts that are often employed to increase stability and photocatalytic destruction of impurities by imparting magnetic characteristics that facilitate separation by an external magnetic field. One of the ferrite compounds  $MgFe_2O_4$  is the n-type semiconductor, has a band gap of 1.7–2.4 eV is chemically and thermally stable (Riyanti *et al.*, 2023).

Cobalt ferrite ( $CoFe_2O_4$ ) is considered a hard-magnetic material among spinel ferrites because of its high  $H_c$ , considerable cubic magneto crystalline anisotropy, and moderate saturation magnetization ( $M_s$ ) (Salih and Mahmood, 2023).  $CoFe_2O_4$  has an inverted spinel structure, meaning that tetrahedral sites contain ferric ions, whereas octahedral sites include ferric and cobalt ions. High curve temperature, temperature stability, low coercivity, high cut-of frequency, high saturation magnetization, low magnetic loss, low magnetic permeability, and biodegradability are among the properties of  $CoFe_2O_4$  (Rekaby *et al.*, 2023). It has been reported that the material displays a number of unique characteristics, including superior electrochemical stability, multiple redox states, excellent permeability, mechanical hardness, ease of synthesis, wear resistance, electrical insulation, high Curie temperature, high coercivity, moderate saturation magnetization, high anisotropy constant, and high magnetostrictive (Tamboli *et al.*, 2023). Lastly, because of its low energy bandgap,  $CoFe_2O_4$  can be used to photocatalytically degrade RhB in the presence of light (Tamboli *et al.*, 2023).

$MnFe_2O_4$ , or manganese ferrite, is one of the most intriguing soft ferrites. It has been widely employed in many different applications, including as electrical devices, medication administration, magnetic resonance imaging (MRI), and many telecommunications sectors. Manganese ferrite is less resistant than other spinel ferrites. The process used to create ferrites may alter how much the crystal structure is inverted (Salih and Mahmood, 2023).

Magnetite,  $Fe_3O_4$ , is a common magnetic iron oxide that is formed via oxygen-iron bonding and has an inverted cubic spinel structure, with Fe (III) ions occupying both tetrahedral and octahedral positions. Because of their many uses and exceptional qualities,  $Fe_3O_4$  nanoparticles are among the most popular magnetic compounds (Ahghari *et al.*, 2023). As an enzymatic antioxidant and one of the most important trace elements in the human body, selenium (Ahghari *et al.*, 2023).

This paper intends to review a number of topics, such as the most significant applications in conventional and modern technologies, as well as the various synthesis methods of metal oxide semiconductors and Spinel ferrites nanoparticles, their benefits and drawbacks.

## II. PHOTOCATALYTIC MECHANISM OF ZnO-BASED COMPOSITES

A photocatalyst in the photocatalytic process absorb photons. Electron/hole pairs are produced by this photoexcitation at the semiconductor surface that is triggered to release hydroxyl radicals, an oxidant that aids in the complete breakdown of organic dyes (Vanitha *et al.*, 2023).

The fundamental idea behind photocatalysis is that it produces  $e^-/h^+$  pairs when excited by a particular wavelength of

light, which can initiate a number of redox reactions on the surface of the catalyst. A schematic of ZnO's photocatalytic mechanism is shown in Fig. 1. The following steps are primarily involved in ZnO photocatalytic reactions: (I) ZnO is excited by light ( $h\nu$ ) equal to or greater than its band gap energy, and the valence band (VB)  $e^-$  absorbs photon energy higher than its band gap to leap from the VB to the conduction band (CB), leaving an unfilled vacancy in the VB called  $h^+$ . (II) photogenerated  $e^-/h^+$  have a strong propensity for mutual extinction and radiative recombination. The  $e^-/h^+$  pairs that survive are moved to the ZnO surface, where they are ensnared by scavengers of  $h^+$  and  $e^-$ , preventing the compounding process. To increase the efficiency of photocatalysis, this is also necessary. (III) Subsequently,  $e^-$  and  $h^+$  undergo reduction or oxidation reactions on the ZnO surface. Superoxide anion free radicals ( $\cdot O_2^-$ ) are created when the  $e^-$  on the CB reacts with oxygen. Next, protonation creates hydrogen peroxide radicals ( $HO_2\cdot$ ), which then react further to produce hydrogen peroxide ( $H_2O_2$ ), and lastly,  $H_2O_2$  reacts with  $\cdot O_2$  to form hydroxyl free radicals ( $\cdot OH$ ). In addition,  $H_2O_2$  reacts with  $h^+$  and  $e^-$  to create additional  $\cdot OH$ . Moreover, VB's  $h^+$  produces  $\cdot OH$  through a reaction with water and hydroxide ions. Strong oxidising agents like  $\cdot OH$  cause pollutants to be reduced to intermediate compounds, which then mineralize into innocuous substances like carbon dioxide ( $CO_2$ ) and water. ROS, such as  $H_2O_2$ ,  $\cdot OH$ , and peroxides, are produced during reactions and have the ability to damage cell structure, which ultimately results in the death of bacteria (Sun *et al.*, 2023).

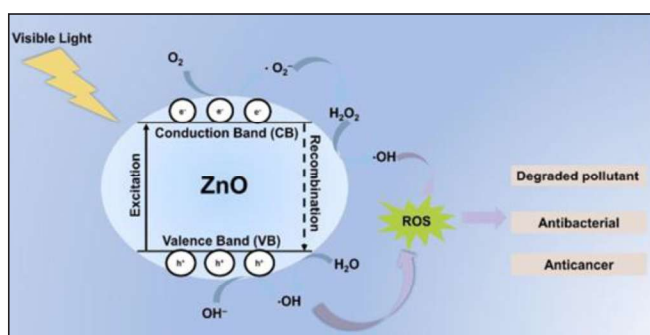
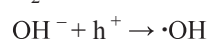
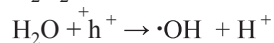
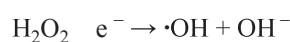
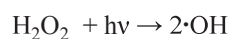
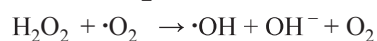
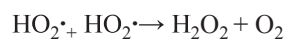
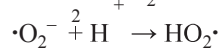
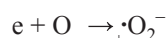
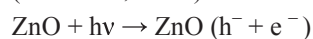


Fig. 1: Schematic Representation of the Photocatalytic Mechanism of ZnO

### III. FACTORS AFFECTING THE SYNTHESIS OF NANOMATERIALS

The synthesis, properties, and uses of nanomaterials are influenced by numerous variables. The size of the synthesised nanoparticles and the rate of reaction are both affected by temperature. As the reaction medium's temperature rises, reaction rate and the size of the nanoparticles also increases. Because some reactions are pH dependent and because aggregation of nanoparticles increases with increasing pH, the size, shape, and concentration of the nanoparticles produced can vary greatly depending on the pH of the reaction medium. Therefore, different types of nanoparticles can be created by adjusting the temperature and pH of the solution. The size and concentration of the synthesised nanoparticle are also largely determined by the reaction time. Up until the reaction ends in solution, the concentration and size of nanoparticles increase with reaction time.

The synthesis of nanomaterials is also influenced by the concentration of precursors. Because the precursors aid in the growth of the nanoparticles, the size and concentration of the nanoparticles increase as the precursor concentration increases. Because the synthesised nanoparticles have a high collision frequency and high surface energy, agglomeration of nanoparticles happens when a high concentration of reactants is used. The amount and nature of solvent affect the synthesis of nanoparticles. Smaller-sized nanoparticles are produced in the reaction medium as the solvent concentration rises, which is attributed to a drop in precursor concentration, an increase in the diffusion constant, and a decrease in growth rate because of less mass transfer in the solution. The polarity, viscosity, and molecular weight of the solvent also affect the synthesised nanoparticles. Additional elements that affect nanoparticles include surfactants, doping materials, and capping agents or ligands (Kokilaa *et al.*, 2022).

### IV. PHOTOCATALYTIC INEFFICIENCY OF THE SEMICONDUCTORS AND SPINEL FERRITES NANOMATERIALS

Depending on the degree of photoetching, semiconductor photocatalysts with strong visible light sensitivity can only be used in limited situations. Firstly, it is unable to fully utilise the light energy in the visible light band due to its large band gap and narrow absorption wavelength range of sunlight. They only act as photocatalysts when exposed to ultraviolet (UV) light because of their large band gaps ( $>3.0$  eV), which only make up 3%–5% of sunlight. Additionally, because the solar spectrum only comprises 4.0% and 45% of UV and visible light, respectively, they are not appropriate for it (Riyanti *et al.*, 2023). Second, before reaching the surface, these semiconductors' broad band gaps cause the electron-hole to recombine with other semiconductors in the bulk of the material. Third, there is a risk of photocorrosion and instability with the photocatalyst itself

Sun *et al.*, 2023). Therefore, creating effective and appropriate photocatalysts that can use visible light and have tiny band gaps to enhance photodegradation processes is a significant task (Bayahia, 2022).

Similarly, there exists a major issue with ferrite nanoparticles which includes low pH requirement, slow degradation kinetics, and high energy consumption of this visible-light-driven photocatalytic degradation of organic dyes (Gupta *et al.*, 2020). After 60 minutes of UV irradiation, only 30–35% of the dye was seen to break down, and it was found that the photocatalytic activity of all four ferrites CoF, NiF, CuF, and ZnF was insufficient when H<sub>2</sub>O<sub>2</sub> was absent. Organic dye photodegradation over ferrite photocatalysts with H<sub>2</sub>O<sub>2</sub> assistance demonstrated quick decolorization at neutral pH.

Due to its high saturation magnetization, nanomaterials containing magnetite (Fe<sub>3</sub>O<sub>4</sub>) have extensively been used. However, oxygen dissolved in the air or water may easily oxidize synthetic magnetite, thereby reducing the saturation magnetization and, thus, the effectiveness of magnetic separation and material life (Oliveira *et al.*, 2022). The use of homogeneous ferrous or ferric salts in industry often has a number of disadvantages, including the production of sludge at the conclusion of the operation, a restricted pH range between 2 and 4 and the deactivation of the catalyst by some agents etc. Furthermore, the expense of treating actual wastewater is increased since the catalysts cannot be recycled.

Of all the synthesis strategies, the synthesis processes play a major role in the usefulness of MFe<sub>2</sub>O<sub>4</sub> in many applications; however, further research is needed to determine the most cost-effective way to synthesise large amounts of MFe<sub>2</sub>O<sub>4</sub> with monodisperse size and shape for biomedical applications. Additionally, it is crucial to consider and carefully investigate the toxicity of particular MFe<sub>2</sub>O<sub>4</sub> NPs (Salih and Mahmood, 2023).

## V. STRATEGIES TO IMPROVE THE PHOTOCATALYTIC EFFICIENCY OF SEMICONDUCTORS AND SPINEL FERRITES NANOMATERIALS

Two main issues were addressed in order to increase the photocatalytic efficiency of metal oxide semiconductors: first, the wide bandgap (3.7 eV) of the semiconductor, which is poor at capturing visible light, leading to a narrow spectral range and small apparent rate constant of photocatalysis. The second factor lowers the ROS yield: the quick recombination rate of photogenerated carriers. Controlling the intended shape, adding more atoms to the lattice, boosting the surface area, and other methods can all be used to increase the photocatalytic activity of metal oxide semiconductors. Several techniques are introduced to increase light harvesting, such as coating, doping with other metals, and semiconductor material (Mousa *et al.*, 2021). In order to achieve spontaneous photodegradation, the addition of another metal helps to lower the band gap and delay the

formation of electron recombination holes provided that metals narrow the bandgap and postpone the electron recombination hole (Mougnol *et al.*, 2022).

Enhancing the photocatalytic performance of metal oxide is most commonly achieved through doping, which is the introduction of elements into a semiconductor's lattice through specific techniques. Metal oxide's visible absorption range can be expanded in three main ways: (i) by raising the VB maximum; (ii) by lowering the CB minimum; and (iii) by adding local energy levels to the bandgap. Doping introduces elements into the ZnO lattice, reducing the band gap of the photocatalyst, increasing its absorption wavelength range, optimising its internal equivalent circuit structure, and increasing the catalyst's activity (Shu *et al.*, 2023) while also producing more active sites. It is a useful tactic to increase the material's electrical conductivity, increase the range of invisible light it can absorb, and boost its catalytic activity.

The ability of zinc oxide (ZnO) doped with several rare earth elements (La, Ce, Pr, Er, Yb) shown the potential for Yb-doped ZnO to function as a stable and effective photocatalyst. Most researchers have focused their attention on ZnO doped with transition metals. According to recent studies on Cu-doped ZnO, Cu is present in the host lattice in the (2<sup>+</sup>) oxidation state, which raises the catalytic activity efficiency (Sun *et al.*, 2023).

Apart from doping with a single element, the study revealed that doping a semiconductor with two or more elements might make up for any shortcomings and result in improved photocatalytic activity. It has been reported that ZnO exhibits a high density of active sites and a lowered charge complexation rate of e<sup>-</sup>/hole pairs when simultaneously doped with sulphur (S) and chlorine (Cl) utilising an ammonium chloride and ammonium sulphide hydrothermal technique. The modified ZnO with a low charge complexation rate of e<sup>-</sup>/h<sup>+</sup> pairs and a high density of active sites and optical band gap can be shrunked from 3.25 eV to 2.9 eV (Sun *et al.*, 2023) and the photocatalytic degradation rate becomes 2.36 times higher than that of pure ZnO. In a similar manner, co-doping with Yb and Ce could alter the crystal structure of ZnO, and the lattice constants rose as the concentrations of these ions increased. By depositing noble metal nanoparticles (such as Ag NPs, Au NPs, Pd NPs, etc.) or noble metal oxides on the ZnO surface, one can enhance ZnO photocatalytic activity and prevent the formation of photogenerated h<sup>+</sup>/e<sup>-</sup> complexes (Sun *et al.*, 2023).

Apart from the aforementioned modification techniques, combining ZnO with semiconductors possessing superior chemical and physical characteristics is another plausible approach to enhance photocatalytic efficiency. The researchers found that when ZnO was coupled to a semiconductor with a low energy band gap, photogenerated electrons would flow from the semiconductor with the higher CB minimum to the one with the lower one when exposed to light. This would improve the separation of h<sup>+</sup> and e<sup>-</sup>, subsequently lengthen the charge carrier lifetime, and decrease the h<sup>+</sup>/e<sup>-</sup> complex. By enhancing

ZnO's photocatalytic potential through this technique, mutual benefits can be maximised or complementary effects can be superimposed (Sun *et al.*, 2023).

A new and effective photocatalytic material may be created by engineering a heterojunction of two semiconductor materials. This helps in increasing the surface area of hydroxide groups by speeding up the transfer of photoinduced charge carriers. The development of heterojunction with varying band gap energy in ZnO@TiO<sub>2</sub> photocatalyst materials synthesized at the nanoscale level has gain interest (Mousa *et al.*, 2021).

Similarly, in the ferrite nanoparticles, instability issue can be taken care of by combining iron oxide with metal ferrite nanoparticles for the oxidation of organic contaminants. It has been observed that combining Fe<sub>3</sub>O<sub>4</sub> with CoFe<sub>2</sub>O<sub>4</sub> and ZnFe<sub>2</sub>O<sub>4</sub> can significantly increase dye degradation photocatalysis. The favourable characteristics are brought about by the surface redox-active centres (B<sub>3</sub><sup>+</sup>/B<sub>2</sub><sup>+</sup> and A<sub>3</sub><sup>+</sup>/A<sub>2</sub><sup>+</sup>) for O<sub>2</sub> adsorption and activation, which are the consequence of electrons bouncing between various valence states of metals at O-sites (Fatimah *et al.*, 2023).

The efficiency of degradation can be improved by combining H<sub>2</sub>O<sub>2</sub> with a photocatalyst consisting of ferrite compounds. For instance, CoFe<sub>2</sub>O<sub>4</sub> was more effectively photocatalytically degraded by H<sub>2</sub>O<sub>2</sub> on rhodamine B dyes than it was when exposed to visible light. Similarly, Fe<sub>3</sub>O<sub>4</sub>+H<sub>2</sub>O<sub>2</sub> photocatalytically degraded naphthalene more effectively than H<sub>2</sub>O<sub>2</sub> alone. Oxidants like H<sub>2</sub>O<sub>2</sub> can produce more hydroxyl radicals, which will boost the rate of deterioration. Furthermore, it poses no hazard and is safe to environment since it readily breaks down into oxygen and water (Riyanti *et al.*, 2023).

CoFe<sub>2</sub>O<sub>4</sub> and CuNiFe<sub>2</sub>O<sub>4</sub> nanoparticle-based magnetic nanoengineered materials have been effectively used as photocatalysts and adsorbents to break down acid dyes on multiwalled carbon nanotubes. Additionally, it has been demonstrated that chitosan polymers coated with Fe<sub>2</sub>O<sub>3</sub> nanoparticles are effective nanomaterials for adsorbing this kind of dye from water (Oliveira *et al.*, 2022).

To remove RBBR from aqueous solutions, an advanced hybrid nanoadsorbent composed of three distinct component materials was used. The core@shell nanoparticles that make up the magnetic portion have a highly magnetic cobalt ferrite core surrounded by a shell of (CoFe<sub>2</sub>O<sub>4</sub>@γ-Fe<sub>2</sub>O<sub>3</sub>) maghemite. Because the cobalt ferrite phase makes magnetic separation simple, the nanoadsorbent is endowed by the maghemite shell, and the CTAB improves the adsorption capacity for both anionic and nonpolar species, this innovative architecture offers a highly suitable nanoadsorbent for RBBR and other anionic dyes (Oliveira *et al.*, 2022).

Although CoFe<sub>2</sub>O<sub>4</sub> is a well-known dye treatment catalyst, its antibacterial activity pales in comparison to that of other nanometals, such as nano-Ag, nano-Au, and nano-Cu. Of these,

silver nanoparticles (Ag NPs) are among the most widely used nanomaterials with antimicrobial properties. The catalytic efficiency of Ag/CoFe<sub>2</sub>O<sub>4</sub> is 3.8 times higher than that of CoFe<sub>2</sub>O<sub>4</sub>. Ag/CoFe<sub>2</sub>O<sub>4</sub> nanoparticles (Ag/CFO NPs) composite, thus, shows promise for the treatment of dye, organic chemical, and bacteria in real wastewater (Hoa *et al.*, 2023).

An efficient and reliable surfactant-mediated co-precipitation approach was utilised to fabricate spinel ferrites (MFe<sub>2</sub>O<sub>4</sub>; M = Co, Ni, Cu, Zn) in order to create new ferrite photocatalysts that may be employed for dye degradation at neutral pH with minimal energy consumption. It was discovered that these ferrite photocatalysts were extremely effective in breaking down various organic dyes at neutral pH in a 32W UV-C/H<sub>2</sub>O<sub>2</sub> system (Gupta *et al.*, 2020).

Visible light may be absorbed by graphite-like carbon nitride (two-dimensional) (g-C<sub>3</sub>N<sub>4</sub>), a polymeric, nonmetal material with a band gap of 2.7 electron volts (eV) that is typical of semiconductors (Hu *et al.*, 2020). Because of its appropriate band gap, excellent stability, and straightforward preparation process, g-C<sub>3</sub>N<sub>4</sub> is primarily utilised in pollutant degradation-related applications. Furthermore, by doping g-C<sub>3</sub>N<sub>4</sub> with metallic or nonmetallic elements or combining it with other organic dyes, researchers have worked hard to increase the efficiency of g-C<sub>3</sub>N<sub>4</sub> photocatalysis (Ali *et al.*, 2023).

## VI. SYNTHESIS OF SEMICONDUCTORS AND SPINEL FERRITES NANOMATERIALS

These metal oxide nanoparticles (NPs) can be synthesized using a variety of methods, some related to the top-down strategy (atomization, laser ablation, radiofrequency, sputtering, etc.) and bottom-up strategy (sol gel process, template synthesis, electro-deposition, microwave-assisted synthesis, etc.). Due to their versatility, simplicity, dependability, and cost-effectiveness, controlled particle size distribution, the hydrothermal, precipitation, colloidal, and sol-gel procedures have been the most widely employed for the synthesis of nanomaterials out of all of these deposition techniques (Luque-Morales *et al.*, 2021).

### A. Hydrothermal Method

Due to its formation of excellent quality crystals of different sizes, the hydrothermal synthesis method of nanoparticles is a rapidly growing procedure. Since the reaction is conducted in a closed system, the hydrothermal process has several advantages over other conventional processes, including reduced operating temperature when the right solvent is present, energy savings, simplicity, cost-effectiveness, improved nucleation control, and pollution-free results. Any homogeneous (nanoparticles) or heterogeneous (bulk materials) reaction in the presence of aqueous solvents at high pressure and temperature to make relatively insoluble materials soluble and recrystallize can be referred to as hydrothermal processing. The hydrothermal method of synthesis allows for the easy production of products

of the intermediate state, metastable state, and specific phase as well as the acquisition of materials that are challenging to synthesis via solid-state reaction. By adjusting particular parameters like the reaction temperature, pressure, solution composition, solvent pH, surfactant concentration, and ageing duration, the hydrothermal synthesising method can modify particle morphology and control grain size, surface chemistry, and crystalline phase. The chemical properties of solvents have the potential to enhance nucleation and grain growth, which in turn can impact the mass and structure of nanoparticles. The size and chemical characteristics can be determined by the solvents' viscosity. Control over structural stability, composition, size, and morphology can be achieved by adjusting the pH of the solution (Kokilaa *et al.*, 2022).

### B. Sol–Gel Synthesis

One of the most flexible techniques for creating various materials at the nanoscale is the sol-gel method. Using this process, a colloidal suspension known as sol is created by hydrolyzing precursors. Liquid sols turn into solid gels due to polymerization. Moreover, a homogeneous, consistent, and ultrafine powder is ultimately acquired. It is an efficient, low-temperature method for creating highly flexible nanoparticles with the desired composition, size, shape, format, and functionalities. This technique is frequently used to synthesise complex metal oxides, temperature-sensitive organic–inorganic

hybrid materials, and thermodynamically unfavourable or metastable materials (Kokilaa *et al.*, 2022).

The five main steps in the sol-gel process are as follows: ageing, drying, hydrolysis, polycondensation, and thermal treatment, also known as calcination (Fig. 2). To create a solution, precursors must first be dissolvable in an appropriate solvent. In the presence of a catalyst and at an appropriate pH, the monomer or starting material in the solution undergoes hydrolysis. A primary condensation reaction then takes place to create a low viscosity solution containing a uniformly distributed colloidal suspension of nanoparticles that undergo Brownian motion, which is referred to as “sol.” The amount of water in a condensation step affects the branching and polymerization levels. Colloidal particles transform into polymeric chains that are dispersed throughout the liquid phase following polycondensation. Over a liquid phase known as “gel,” a continuous structure is formed by an interconnected web of solid-phase particles. During the ageing and drying processes, polycondensation takes place and the gel’s strength grows; the extra solvent is eliminated. Lastly, calcination is used to eliminate solvent molecules and residues from the necessary product. It also keeps the temperature at the right level, regulating the final product’s pore size and density. High-purity materials in the forms of powders, fibres, monoliths, self-supported bulk structures, and thin-film coatings can be synthesised using the sol–gel process (Kokilaa *et al.*, 2022).

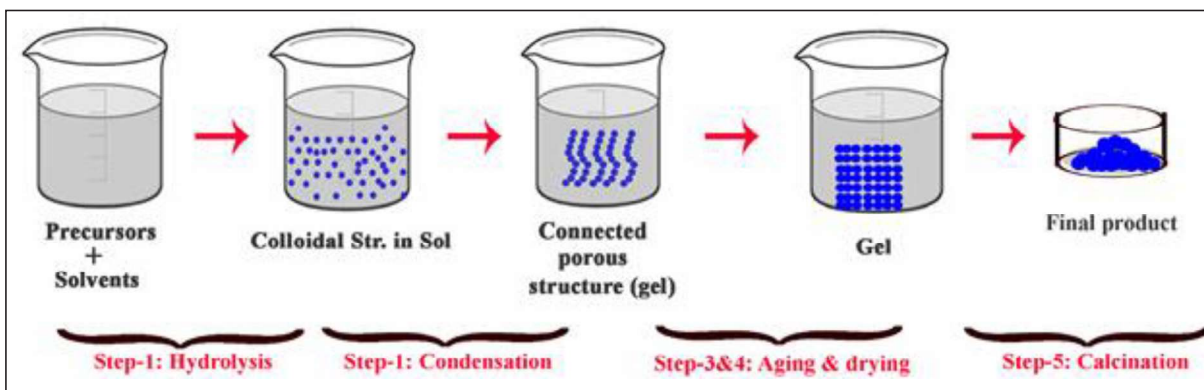


Fig. 2: Graphical Representation and Different Process Involved in Synthesis of Nanomaterials by Sol–Gel Method

Scaling up the product is challenging with the sol–gel process, which uses a lot of energy. Acoustic cavitation is incompatible with materials that are heat-sensitive. Sonochemical synthesis requires a comparatively large energy supply, resulting in a low yield per unit of energy supplied.

### C. Chemical Vapor Deposition

A widely used material-processing deposition technique called chemical vapour deposition (CVD) involves settling down nonvolatile thin solid films or crystals on a preheated supporting substrate, usually under vacuum. The foundation of CVD is the solid-vapor phase precursor chemical reaction that

takes place upon the deposition of vapour precursor on a hot solid substrate of choice. Certain species of gaseous reactants have the potential to undergo reactions and form intermediate reactants. These original raw reactants or intermediate reactants can be absorbed and diffused onto a substrate that has been heated enough, and they can then go through a solid-gas interface reaction to nucleate, grow, and coalesce to deposit the desired thickness of the film or coatings. The process of the CVD mechanism can occur in an open reactor system with an inert gas flow or in a closed reactor system. A closed reactor system containing the precursors is filled and securely closed. The chemical reaction is then brought about by applying a differential temperature; however, in an open reactor system,

precursors are continuously introduced into the reactor with the assistance of carrier gas (Kokilaa *et al.*, 2022).

Sublimation or first dissolution in an appropriate solvent is required for solid precursors. Either direct gas reactants are used, or liquid precursors or solutions containing solid precursors evaporate to the gaseous phase before being absorbed on the substrate. Nitrogen gas or inert argon is examples of carrier gases that are used to move these gaseous reactants into reaction chambers. In CVD, both hot-walled and cold-walled reactors are utilised. Compared to physical and other conventional vapour deposition methods, the CVD method of synthesis offers many advanced advantages. These advantages include conformal film deposition of varying thickness, uniform film deposition with less porosity, high stability, purity, and complex final product. The CVD method is altered in a number of ways to remove certain restrictions and produce a final product with the desired properties. Several techniques include atmospheric pressure CVD, ultra-high vacuum CVD and low pressure CVD, laser-enhanced CVD, plasma-enhanced CVD (PECVD) or plasma-assisted CVD, and altering different reaction conditions and elements like substrate, temperature, pressure, and precursor composition in different nanoparticle sizes and shapes with desired properties (Kokilaa *et al.*, 2022).

#### D. Green Synthesis

It is pertinent to mention that the physical and chemical processes used to create metal oxide have proven to be expensive and hazardous. Green synthesis is one such approach that shows the most promising to resolve these problems. The environmentally friendly production of

metal-based nanoparticles involves the extraction of various plant components, such as leaves, stems, bark, flowers, microbial and root synthesis, which is a safe substitute for the environment. Numerous secondary metabolites, biomolecules, and phytochemicals such as phenolics, alkaloids, flavonoids, saponins, proteins, peptides, tannins, terpenoids, and volatile oils are found in the majority of plants in nature. These phytochemicals' functional groups act as capping, stabilising, and reducing agents to promote the production of NPs (Bhardwaj and Singh, 2023). They need less energy to produce and stop the aggregation of nanoparticles. These phytochemicals create a coating on the catalyst that inhibits agglomeration and results in the time-dependent stability of synthesised nanoparticles (Luque-Morales *et al.*, 2021; Mognol *et al.*, 2022; Taymaz *et al.*, 2023; Rathi *et al.*, 2023).

The synthesis of metal nanoparticles (NPs) has been documented in multiple reports utilising leaf extracts from various plants, including *Phyllanthus amarus*, *Thymus vulgaris*, *Citrus Limetta*, *Hardwickia binata* leaves, *Aquilegia pubiflora*, *Cananga odorata* essential oil, leech peel, *Hardwickia binate*, *Moringa oleifera* seed, cow bones, groundnut shells, *Lactobacillus* spp, *G. cambogia* fruit (Fig. 3). The production of nanoparticles using plant extracts from various plant species has been a common application for silver (Ag), copper (Cu), gold (Au), zinc (Zn), and many other metals. By using ecological agents and producing fewer hazardous byproducts, these techniques help to improve environmentally friendly processes and make them faster, safer, cheaper, and simpler (Luque-Morales *et al.*, 2021; Nabi *et al.*, 2021; Mognol *et al.*, 2022; Taymaz *et al.*, 2023; Rathi *et al.*, 2023; Manimegalai *et al.*, 2023; Bhardwaj and Singh, 2023).

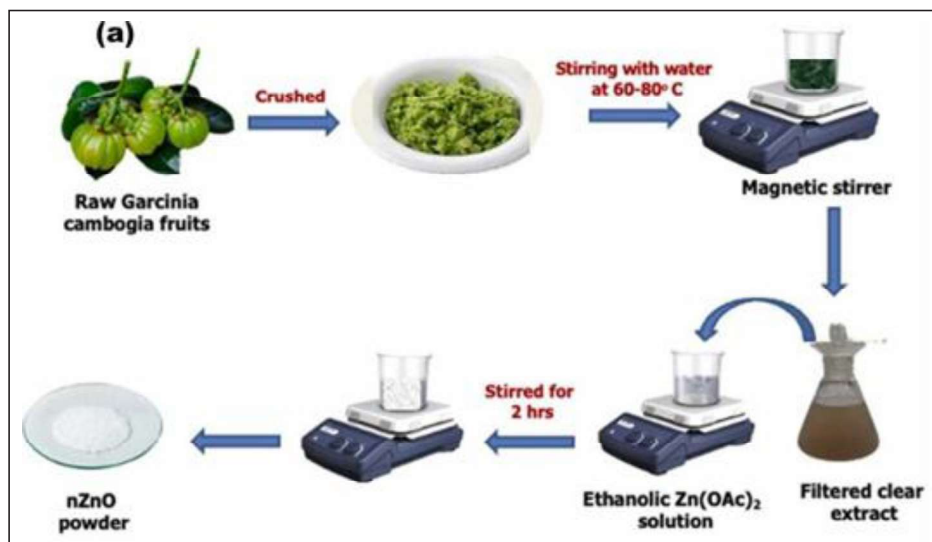


Fig. 3: Schematic Representation ZnO NPs Synthesis via Green Synthesis Route Using G. Cambogia Fruit

#### E. Synthesis of Spinel Ferrite

MFe<sub>2</sub>O<sub>4</sub> NPs can economically be synthesised using co-precipitation. This process produces spinel ferrite nanoparticles

(NPs) with a homogenous structure, high purity, and adjustable size. In Salts (sulphates, chlorides, or nitrates) are combined with a base, which serves as a precipitating agent, at temperatures

high enough to cause precipitation. The size, form, and characteristics of spinel ferrite NPs are influenced by a number of variables, including pH, temperature, reaction duration, and the kind and ratio of precursors (Salih and Mahmood, 2023). The primary challenge with co-precipitation NP preparation is their poor crystallinity, which may be addressed with a subsequent heat treatment.

Similarly, for the ferrite nanoparticles, numerous wet-chemical procedures are used in hydrothermal and solvothermal syntheses to produce crystalline  $\text{MFe}_2\text{O}_4$  magnetic nanoparticles. It is possible to generate MNPs with a controlled shape and high purity using straightforward and efficient solvothermal and hydrothermal processes. It makes use of a nonaqueous solution, such methanol, ethanol, or ethylene glycol. To dissolve the metal precursors in solvothermal synthesis at a moderate temperature and high pressure (Salih and Mahmood, 2023).

The fundamental drawback of the sol-gel process, despite its simplicity and inexpensive cost, is its lack of purity in the end product. Thermal treatment is required to attain high purity and crystalline nanoparticles. The kind of precursors present in the initial colloidal solution has a considerable impact on the form and crystallinity of the nanoparticles created using this approach.

The co-precipitation method's size and morphological limitations are overcome by the thermal decomposition method. Generally speaking, magnetic nanoparticles generated at higher temperatures have more homogenous size distributions. In addition, high-temperature breakdown can be used to create more crystalline  $\text{MFe}_2\text{O}_4$  MNPs. With this technique, spinel ferrite NPs may be made into a variety of forms, including cubic and octahedral, by varying the temperature, heating rate, concentration of organic substances, and kind of organic solvent. Because of its high crystallite and narrow size distributions, thermal breakdown of spinel ferrite NPs is a more favourable approach for biomedical applications than co-precipitation production (Salih and Mahmood, 2023).

Using the coprecipitation method, a new nanocomposite known as (MnCr)-LDO<sub>5</sub> wt%/CoFe<sub>2</sub>O<sub>4</sub> was effectively created. Its methyl orange dye removal effectiveness was investigated and contrasted with that of pure CoFe<sub>2</sub>O<sub>4</sub>. Numerous factors were investigated, including contact duration, dye concentration, dose of the nanoadsorbent, and pH to demonstrate their impact on the MO adsorption process. The highest removal percentage for 25 ppm of MO by 0.1 g/100 mL of (MnCr)-LDO<sub>5</sub> wt%/CoFe<sub>2</sub>O<sub>4</sub> at pH 3 was found to be 86.1%. Batch conditions were used for isotherm and kinetics investigations. The primary method of MO removal by CoFe<sub>2</sub>O<sub>4</sub> nanoadsorbent is physical adsorption, whereas the (MnCr)-LDO<sub>5</sub>wt.%/CoFe<sub>2</sub>O<sub>4</sub> nanoadsorbent was influenced by both physical and chemical adsorption processes (Rekaby *et al.*, 2023).

Using inexpensive materials with a high surface area to volume ratio can also help to enhance it. According to Oliveira *et al.* (2022), metal hydroxides derived from in situ electrosynthesis have shown promise as adsorbents in the removal of organic contaminants from water.

By applying an electric field, bismuth ferrite (BFO) nanoparticles (NPs) can regulate their magnetic characteristics since they exhibit both canted magnetic and ferroelectric behaviour concurrently in a single-phase compound. This magnetoelectric characteristic opens up new technical possibilities in information storage and spintronics. Together with sensing apparatus (Jamshaid *et al.*, 2022).

Because of their superior photocatalytic efficacy and reduced band gap, which is observable, BFO NPs also attract attention. Research shows that doping BFO NPs at the A and B sites with clay mineral and cobalt metal ions, respectively, can enhance their structural, magnetic, and characteristics of bismuth ferrites' dielectric. Additionally, Bent-Co-doped BFO NPs improved the photocatalytic activity, suggesting that they might be used as a photocatalyst to remove harmful colours from textile effluents, such as methyl orange (Jamshaid *et al.*, 2022).

Green chemistry researchers use natural resources such as plants, plant-derived products, and microorganisms (bacteria, fungus, yeast, algae, etc.) that reduce pollution and environmental dangers at the beginning of chemical processes, enhance human health, and save the environment. Cobalt ferrite nanocomposites was synthesised in an environmentally friendly manner using honey. Honey has several benefits as a lowering and stabilising agent. It is possible to stop nanoparticle agglomeration by stabilising superparamagnetic cobalt-zinc ferrites nanoparticles by honey-mediated synthesis and ginger/cardamom extracts (Tamboli *et al.*, 2023).

Different plant extracts have been used as reducing agents in the synthesis of Ag NPs. There are a lot of polyphenols in jasmine flower tea. Among plants like blueberries, pomegranates, mangoes, mint, peaches, and lemons, jasmine has been demonstrated to have the strongest antioxidant and anticancer properties (Hoa *et al.*, 2023).

## VII. CHARACTERIZATION

Before using synthesised nanoparticles in different applications, they must first be thoroughly characterised. While there are numerous analytical methods for characterising new nanoparticles, UV-visible spectroscopy is frequently employed to verify the creation, stability, and aggregation of nanoparticles. FTIR (Fourier-transform infrared) spectroscopy provides information on atomic arrangement, functional groups, and surface chemistry. Microscopic techniques such

as transmission electron microscopy (TEM), high resolution transmission electron microscopy (HR-TEM), scanning electron microscopy (SEM), field emission scanning electron microscopy (FE-SEM), atomic force microscopy (AFM), and dynamic light scattering (DLS) are commonly used to determine the morphology, topography, size, and size distribution of nanoparticles. X-ray fluorescence (XRF) and energy-dispersive X-ray spectroscopy (EDX) are frequently used to examine the composition and elemental components of nanomaterials. Nanomaterials' elemental composition and different forms of crystallinity can be ascertained using X-ray diffraction (XRD). UV-visible, photoluminescence (PL), and null ellipsometer optical instruments are used to determine optical properties. Thermogravimetric analysis (TGA) is a common method used to examine thermal properties. The primary applications of X-ray photoelectron spectroscopy (XPS) are surface analysis and confirmation of the composition and elements contained in nanomaterials (Kokilaa *et al.*, 2022).

The diffraction pattern clearly shows the characteristic peaks of this material, which are located at 31.74, 34.38, 36.22, 47.55, 56.54, 62.81, and 67.85  $2\theta$ . These values correspond to the Miller indexes of (100), (002), (101), (102), (110), (103), and (112), respectively. These peaks align with JCPDS Card No. 76-0704's, which depicts the ZnO-NPs as hexagonal structures wurtzite type zinc. The plant extract method produced ZnO particles with a high degree of purity and crystallinity since no additional peaks were detected in the spectra, indicating the absence of impurities. FTIR reveals that the ZnO-NPs contain functional groups such as alcohol, anhydrides, carboxylic acids, and primary amines. SEM and TEM studies verified the spherically shaped morphology (Luque-Morales *et al.*, 2021; Luque-Morales *et al.*, 2021).

The Diffuse Reflectance Spectroscopy (DRS) method was used to show the absorption profile and optical properties of the nanoparticles. ZnO nanoparticles have an absorption-band-edge at 100 nm, corresponding to a band gap energy of 2.9 eV. The resultant carbon from the incomplete combustion of the precursor is responsible for the lowering of the optical band gap when compared to the commercial version (3.7 eV). The synthesised ZnO exhibits a reduction in band gap and a change in wavelength, increasing its catalytic activity to detectable levels (Hosny *et al.*, 2023).

Through the photodegradation of both cationic and anionic dyes under UV light, the photocatalytic activities of the synthesised ZnO-NPs were assessed. One type of anionic dye that was used was fluorescein dye, and a cationic dye was Rhodamine B. The photocatalytic performance of carbon-doped ZnO was significantly impacted by the presence of benzoquinone, ammonium oxalate, and isopropanol. This suggests that hydroxyl radicals, positive holes, and superoxide radicals are involved in the degradation of RhD and Flu dyes (Hosny *et al.*, 2023).

The purity and crystallinity of the magnetic nanoparticles were assessed by XRD analysis. The planes at 30.19°, 35.55°, 43.13°, 53.95°, 57.70°, 62.64°, and 74.95° were the locations where the MgFe<sub>2</sub>O<sub>4</sub> XRD pattern at  $2\theta=10-90^\circ$  was detected. The cubic spinel structure is seen in (220), (311), (400), (422), (511), (440), and (553). Using the Debye-Scherrer formula on the (311) reflection plane, the size of the crystallite of MgFe<sub>2</sub>O<sub>4</sub> was determined to be 14.38 nm. The wavelength range of the catalyst that is absorbing light is shown by the UV-DRS spectra. 420 nm is the wavelength at which the highest absorption is seen, suggesting that MgFe<sub>2</sub>O<sub>4</sub> is better suited for employment as a catalyst in the visible light spectrum (Riyanti *et al.*, 2023).

Agglomeration occurs in some of the MgFe<sub>2</sub>O<sub>4</sub> particles, giving the material an apparent non-uniform shape. According to SEM mapping, Fe (blue) dominated the surface, Mg (red) was spread nearly equally, and Fe covered the oxygen (O) (Riyanti *et al.*, 2023).

EDS, SEM and TEM were employed to investigate the structural characteristics, particle size, and morphology of each MFe<sub>2</sub>O<sub>4</sub> photocatalyst. This demonstrated that while the many nanoparticle kinds are unique, the spherical-like structures of each type are uniform. Every MFe<sub>2</sub>O<sub>4</sub> sample had a uniform size and was almost spherical (Bayahia, 2022).

The morphologies, textural characteristics, and optical properties of MFe<sub>2</sub>O<sub>4</sub> (where M = Zn, Co, Cu, and Ni) were investigated in addition to its photocatalytic capacity to destroy CV dye. The process of surfactant-mediated co-precipitation was employed to manufacture photocatalysts. The band gaps varied from 1.69 eV to 2.55 eV, while the particle sizes varied from 18 to 32 nm. Under sunny and neutral circumstances, the photodegradation function of each photocatalyst was assessed against CV dye. pH (Bayahia, 2022).

SEM, or scanning electron microscopy, was used to characterize the morphology of ferrite photocatalysts. All four of the photocatalysts—CoF, NiF, CuF, and ZnF—exhibited morphology resembling coral in SEM micrographs. CoF photocatalyst EDS analysis was conducted at the appropriate keV levels (Gupta *et al.*, 2020). The consistent distribution of constituent elements in CoF was confirmed by the 2D elemental mappings, indicating the homogeneity of the photocatalyst. High-resolution transmission electron microscopy was used to better study the morphology of ferrites (HRTEM). For each of the four ferrites, single crystals were found (Gupta *et al.*, 2020).

In SEM, all four of the photocatalysts CoF, NiF, CuF, and ZnF exhibited coral resembling morphology. High-resolution transmission electron microscopy was used to better study the morphology of ferrites (HRTEM). For each of the four ferrites, single crystals were found (Gupta *et al.*, 2020). The elemental makeup and oxidation states of ferrite photocatalysts were ascertained using X-ray photoelectron spectroscopy (XPS)

investigation. The ferrites' XPS full scan spectra verified the presence of major essential components (Gupta *et al.*, 2020).

Two separate vibration bands for MO can be seen in the FTIR spectra of the  $MFe_2O_4$  nanostructures at  $\nu_1$  561.31–603.53  $cm^{-1}$  and  $\nu_2$  418.66–472.03  $cm^{-1}$ . These represent the stretching vibration of the MO bond in the  $MFe_2O_4$  spinel nanoparticles. The  $\nu_1$  band shows the stronger vibration modes of metal and oxygen in tetrahedral structures, while the bottom band shows the stretching vibration mode of oxygen and metal ions ( $Fe_3^+$ ) in octahedral structures (Bayahia, 2022).

The first analysis of the  $Fe_3O_4/Se$  nanocomposites was performed using EDX. The existence of strong peaks associated with O, Fe, and Se stands for nanocomposite elements (3). The effect of the composited components on the overall crystal structure was confirmed by analysing the X-ray diffraction (XRD) pattern of the synthesised  $Fe_3O_4/Se$  nanocomposite. The magnetite  $Fe_3O_4$  NPs diffraction planes (111), (220), (3 1 1), (400), (4 2 2), (511), (4 4 0), and (533) were matched by the diffraction peaks at  $2\theta=18.36, 30.2, 35.5, 43.1, 57.1, 62.7,$  and  $74.3$ . According to Ahghari *et al.* (2023), the  $Fe_3O_4/Se$  NPs' XRD data showed that the  $Fe_3O_4$  core's crystal arrangement remained unchanged during the functionalization process.

The magnetic properties of the  $Fe_3O_4/Se$  hybrid catalyst were ascertained by VSM analysis. There was no hysteresis loop seen in the S-like magnetization curve, indicating that the coercivity ( $H_c$ ) and remanence ( $M_r$ ) Se stands for components of a nanocomposite (3). The X-ray diffraction (XRD) pattern of the  $Fe_3O_4/Se$  nanocomposite was analysed to establish the superparamagnetic nature of this hybrid catalyst and to assess the effect of ( $H_c$  were zero) (Ahghari *et al.*, 2023).

Through XRD analysis, the creation of  $g-C_3N_4$  nanosheet structures, the cubic phase of  $Fe_3O_4$ , and  $g-C_3N_4/Fe_3O_4$  nanocomposites were verified.  $Fe_3O_4$ ,  $g-C_3N_4$ , and their composites were seen to have rod-like structures in SEM micrographs. Because of its high electron mobility, this structure is useful for photocatalysis as exposed to visible light, the magnetically separated  $g-C_3N_4/Fe_3O_4$  catalysts' photocatalytic activity (PCA) increased by up to 1.8 times for MB dye as compared to the unadulterated  $g-C_3N_4$ .  $g-C_3N_4$  has a layered structure with respect to the weak van der Waals between graphite layers, but the planar bonding assembly is entirely different (Ali *et al.*, 2023).

## VIII. APPLICATIONS OF SEMICONDUCTORS AND SPINEL FERRITES NANOMATERIALS

Fig. 4 displays  $MFe_2O_4$ 's most common uses (where  $M = Co, Cu, Mn, Ni,$  and  $Zn$ ). The structure, particle size, and shape of ferrite vary depending on the type of cation and the synthesis method; these changes also affect the ferrite's properties, which further lead to various applications.



Fig. 4: Application of Nanosized Ferrites

### A. Magnetic Applications

The changes in the exchange interaction between the tetrahedral and octahedral sites cause the magnetization to depend on grain size [20, 113]. The magnetic particles should be nanosized for their use in high-density magnetic recording in order to inhibit the exchange interaction between neighbouring grains and lower media noise in the materials. To achieve a high storage density, the particles also need to have high HC values [98]. The octahedral and tetrahedral sites' cationic distribution, composition, crystal structure, and particle size all affect the spinel ferrites' magnetic properties (MR, MS, and HC). Additionally, they might behave in paramagnetic, ferrimagnetic, and antiferromagnetic behaviour. Excellent characteristics of the ferrimagnetic ceramic  $CoFe_2O_4$  include high K, HC, and TC values, moderate MS values, and a large magnetostrictive coefficient value. When the temperature drops below the Néel temperature,  $ZnFe_2O_4$  exhibits antiferromagnetic behaviour; at nanoscale particle sizes, it exhibits diamagnetic, superparamagnetic, or ferrimagnetic behaviour. The combination of several elements, including super-exchange interaction, magneto crystalline anisotropy, canting effect, and dipolar interactions on the NP's surface, is responsible for the magnetic properties of  $NiFe_2O_4$  NPs. Moreover, the domain structure, critical size, and anisotropy of the crystal can all be used to explain how the HC value varies with particle size. Current Developments in  $MFe_2O_4$  Synthesis and Applications (Dippong *et al.*, 2023).

### B. Photocatalytic Applications

Photocatalysts are essential materials that facilitate the use of solar energy in oxidation and reduction processes. They find use in a variety of processes, including the inactivation of cancer cells, the removal of air and water pollutants, odour control, bacterial inactivation, and water splitting for hydrogen production. These days, photocatalysis is the treatment of

choice for removing dyes because, in addition to using light to irradiate a semiconductor, the electron-hole pairs that are created are also utilised for the oxidation and reduction process. Few substances have the dual properties of photo-oxidation and photo-reduction, which allow them to effectively absorb visible light while also completing the breakdown of dangerous organic compounds (Dippong *et al.*, 2023).

ZnO in nanoforms is a useful substance that is widely applied in the photodegradation of different organic contaminants. ZnO NPs quickly and totally degrade MB dye when exposed to UV light. The primary oxidising species that are essential to the photodegradation of toxic compounds (pollutants) are superoxide anions and hydroxyl radicals. Photocatalysis is a dynamic process that initiates a series of redox (reduction and oxidation) reactions simultaneously on the surface of ZONSSs and breaks down the long chain of toxic compounds into smaller fragments, i.e. atoms. Additionally, ZnO NPs were utilised to look into the photocatalytic breakdown of methyl orange (MO). Compared to doped ZnO, ZnO is a better option for catalytic applications. They went on to say that first order kinetics applied to the degradation of MO. Since ZnO has a wider band gap, poor charge separation, a problem with electron hole recombination, and limited light absorption, it has relatively low photocatalytic efficiency. To solve these issues, doping, thermal annealing, and heterojunction photocatalysis are employed. By enhancing ZONSSs' optical and electrical qualities as well as their chemical and physical stability, these techniques raise their functional behaviour.

Ferrites' low crystallite size increases their surface area and number of reaction sites, which boosts their photocatalytic activity. The most crucial elements that improve the photocatalytic properties are the kind of photocatalyst, crystallinity, size of NPs, accessibility of the active surface to contaminants, and diffusion resistance of organic pollutants. Consequently, because of their higher specific surface area and active sites that enhance the photocatalytic activity, small particle sizes with high crystallinity are very desirable.

As a result of their visible light-absorbing band gap and spinel crystal structure, ferrites can be used as photocatalysts to degrade a variety of pollutants [151].  $\text{CoFe}_2\text{O}_4$  was employed as a photocatalyst because of its chemical stability and narrow bandgap (1.1–2.3 eV), which made it active in visible light, for the degradation of organic dyes, such as methylene blue (MB) and rhodamine B (RhB). It was discovered that  $\text{CuFe}_2\text{O}_4$  photocatalyst was more efficient than  $\text{ZnFe}_2\text{O}_4$  and  $\text{NiFe}_2\text{O}_4$  at breaking down dangerous dye compounds. This is most likely because of its large surface area, small band gap, lower crystallite size, and presence of pores that trap oxygen molecules and generate a lot of oxidising species and OH radicals. Under visible light, the photocatalyst was recovered using a magnet and used four times in a row. Under Xe lamp irradiation,  $\text{CuFe}_2\text{O}_4$  "oversized" nanostructures showed enhanced photocatalytic activity in the conversion of benzene.

Furthermore, because of their large surface area ( $\sim 120 \text{ m}^2/\text{g}$ ),  $\text{CuFe}_2\text{O}_4$  powders demonstrated a good catalytic efficiency ( $\sim 60\%$ ) at 200 C and  $\text{pH} = 12$ . It has been reported that the coprecipitation method of photocatalytic ozonation of dyes with  $\text{CuFe}_2\text{O}_4$  NPs can effectively decolorize and degrade textile dyes without the need for high oxygen pressure or heating.  $\text{ZnFe}_2\text{O}_4$  NPs' photocatalytic activity is dependent on their surface characteristics and flaws. Because of  $\text{ZnFe}_2\text{O}_4$ 's comparatively small band gap energy (1.9 eV), strong visible-light response, good photochemical stability, and low-cost. It was also reported that  $\text{ZnFe}_2\text{O}_4$  NPs were used for the photocatalytic degradation of 4-chlorophenol and that the size and shape of the particles affected the efficiency of the degradation. It was discovered that  $\text{ZnFe}_2\text{O}_4$  was a suitable visible-light-driven catalyst because of its small particle size and narrow size distribution, which quickly and completely degraded the RhB dye (Dippong *et al.*, 2023).

## IX. CONCLUSIONS OR IMPORTANT OUTCOME

Titanium dioxide (TiO) and zinc oxide (ZNO) are the most promising options among semiconductor photocatalysts for removing water contaminants because of their low cost, non-toxicity, and long-term stability. One important parameter that affects photocatalytic activity is band gap energy, which is mostly determined by the morphology, crystal structure, and chemical makeup of the materials. By doping the semiconductors with the right foreign elements, band gap energy could be reduced.

In order to achieve higher removal efficiency, it was found that applying agricultural wastes was a better option than using metals. Complex heterogeneous photocatalysts were created, and their oxygen content caused the band gap to narrow and the electron recombination to be delayed (Mougnol *et al.*, 2022). The leaf extract's saponins, phenols, and flavonoids have been found to function as stabilising and reducing agents in addition to reducing agents. The average crystallite size increases with the quantity of leaf extract added to the synthesis medium. The ZnO and  $\text{TiO}_2$  NPs' narrowing bandgap, high crystalline structure, and almost hexagonal morphology are responsible for the enhanced photocatalytic degradation (Taymaz *et al.*, 2023).

In some dye-contaminated water, these Fenton, Fenton-like, and photo-Fenton processes are quite efficient.  $\text{Fe}_3\text{O}_4$  and  $\text{NiFe}_2\text{O}_4$  have been extensively researched for their ability to reduce organic pollutants, such as dyes and pharmaceutical waste, due to their magnetic and band gap energies (Fatimah *et al.*, 2023).  $\text{Fe}_3\text{O}_4$  shown strong photoactivity for phenolic compounds across a broad pH range. It also demonstrated great dye removal efficiency for certain dyes, such as congo red, methylene blue (100%), and RhB (90%).  $\text{NiFe}_2\text{O}_4$  has also been reported to be useful for catalytic oxidation of some substances, including colours and carbon monoxide.  $\text{NiFe}_2\text{O}_4$  has strong photoactivity for the photooxidation of tetracycline, methylene blue, and rhodamine B when exposed to UV light.

These iron oxides' ease of separation, reusability, and stability are important characteristics that contribute to the advanced oxidation process' efficacy (Fatimah *et al.*, 2023).

It has been shown that when  $MFe_2O_4$  nanoparticles were created using the CTAB-mediated co-precipitation-oxidation technique, they exhibited outstanding photocatalytic activity. The concentration of dye, the pH of the solution, and the presence of  $H_2O_2$  all have an impact on the photocatalytic degradation efficiency. The solution pH of 6, the dye concentration of 10 mg/L, the concentration of 2.5 mM  $H_2O_2$ , and the irradiation period of 6 were found to be optimal for photocatalytic degradation. Because the degradation efficiency is above 90% after five cycles,  $MgFe_2O_4$  has great stability and reusability (Riyanti *et al.*, 2023).

The cubic symmetry of CoF, NiF, and ZnF with crystallite sizes between 27 and 36 nm was verified by XRD and TEM investigation. CuF nanoparticles with a crystallite size of 16 nm were in tetragonal symmetry. According to Gupta *et al.* (2020), all of the ferrites absorbed well in the UV, Vis, and NIR range and had an impact on the photocatalytic degradation of organic dyes at neutral pH levels. The production of holes and  $\bullet OH$  radicals in the UV/ $H_2O_2$ /ferrite system was the main mechanism driving dye degradation, as proven by fluorescence spectroscopy. According to the study's findings, under low power UV-C irradiation, these photocatalysts may be employed to treat wastewater polluted with dyes at a reasonable cost without changing the pH (Gupta *et al.*, 2020).

Green synthesis, or the use of natural resources to create nanoparticles, is a cutting-edge and rapidly developing field in the search for more ecologically friendly ways to produce nanoparticles. A more promising method than traditional methods is to synthesise nanoferrites using plant extracts or microorganisms (Tamboli *et al.*, 2023).

## X. SCOPE OF FURTHER RESEARCH

Selection of photocatalysts remains a problem that cannot be disregarded, since different photocatalysts here have different photoelectrochemical properties (Shu, 2023). In general, we take into consideration the photocatalysts' band gap, carrier separation efficiency, and recombination efficiency the most. Particularly, because of their fast electron-hole recombination, which frequently results in a lower quantum yield, and poor photocatalytic performances, these heterogeneous photocatalysts are not as practical under direct sunlight irradiation and therefore have room for improvement in terms of their photocatalytic efficiency (Karthikeyan *et al.*, 2020).

Zinc oxide is a significant wide band gap semiconductor material with a wide range of useful applications. However, the stability and efficiency of zinc oxide performance frequently cannot meet the requirements of practical devices during the preparation process due to the difficulty in controlling vacancies and defects, which affects the application range of nano zinc

oxide. Thus, in recent years, scientific researchers have turned their attention to the introduction of another material onto the surface of zinc oxide as well as the expansion of zinc oxide's application field (Shu, 2023).

Although using greenly produced bio-waste mediated ZnO NPs for photocatalytic dye degradation has several benefits, there are still some important issues that need to be addressed. For example, i) Large-scale synthesis of nanoparticles with repeatability in size and shape and consistency in reactivity, ii) Phytochemicals in the Natural resource materials and bio-waste extract are essential for the production of stabilised ZnO NPs, iii) majority of studies only report photocatalytic efficacy and metal oxide NPs synthesis at the lab scale, iv) worry about the toxicity of the products generated after the dye degradation process and the possibility of secondary pollution required an in-depth investigation during the large-scale application of NPs in real environmental fields (Bhardwaj and Singh, 2023).

Nanoscale spinel ferrites have attracted a lot of attention for the application in the sectors of biomedicine, catalysis, water treatment, and energy due to their suitable properties combined with common functionalizations and modifications. It is evident that the future trend in applications for magnetic spinel ferrites will centre on manipulating the necessary magnetic characteristics by altering the synthetic techniques, adjusting the particle's size, shape, and crystallinity. Effective magnetic materials for magnetic hyperthermia is one use for magnetic spinel ferrites. It is still early in the research phase, and further investigation is required to address some issues such adjusting the size, shape, and magnetic characteristics of nanoparticles. To create magnetic ferrite, one of the most crucial problems to be addressed in the future is the effective ways of surface modification of spinel ferrites nanoparticles with anticipated biological application performance (Salih and Mahmood, 2023).

While there is great potential for green synthesis of nanoscale cobalt ferrite, there are a number of obstacles and disadvantages to consider. These include the requirement to find appropriate synthesis conditions, control over the quantity and quality of the final product (low purity and poor yield), identify specific applications, and choose and obtain specific materials (complex extraction processes, seasonal and regional availability of raw materials and their compositions). These limitations present challenges for the practical use of green-synthesised nanoscale cobalt ferrite as well as for large-scale production adaptability/reproducibility (time and location of production). So, selecting the best natural resource (a cheap and commercially available raw material), employing large-scale feasible synthesis conditions, focusing on yield improvement, achieving appropriate quality and size of nanoparticles, and later on utilising simple energy-saving technology are some of the research directions that need to be looked into. The green synthesis of nanoscale cobalt ferrite is therefore expected to have a bright future and significant development potential (Tamboli *et al.*, 2023).

## REFERENCES

- [1] M. R. Ahghari, Z. Amiri-Khamakani, and A. Maleki, "Synthesis and characterization of Se doped  $\text{Fe}_3\text{O}_4$  nanoparticles for catalytic and biological properties," *Scientific Reports*, vol. 13, Jan. 18, 2023, Art. no. 1007. [Online]. Available: <https://www.nature.com/articles/s41598-023-28284-x>
- [2] A. Ali, M. Amin, M. Tahir, S. S. Ali, A. Hussain, I. Ahmad, A. Mahmood, M. U. Farooq, and A. M. Farid, " $\text{g-C}_3\text{N}_4/\text{Fe}_3\text{O}_4$  composites synthesized via solid-state reaction and photocatalytic activity evaluation of methyl blue degradation under visible light irradiation," *Frontiers in Materials*, vol. 10, May 09, 2023. [Online]. Available: <https://www.frontiersin.org/journals/materials/articles/10.3389/fmats.2023.1180646/full>
- [3] H. Bayahia, "High activity of  $\text{ZnFe}_2\text{O}_4$  nanoparticles for photodegradation of crystal violet dye solution in the presence of sunlight," *Journal of Taibah University for Science*, vol. 16, pp. 988-1004, Apr. 18, 2022. [Online]. Available: <https://www.tandfonline.com/doi/full/10.1080/16583655.2022.2134696>
- [4] E. Brillas, and S. Garcia-Segura, "Recent progress of applied  $\text{TiO}_2$  photoelectrocatalysis for the degradation of organic pollutants in wastewaters," *Journal of Environmental Chemical Engineering*, vol. 11, no. 3, Jul. 17, 2023. [Online]. Available: <https://www.sciencedirect.com/science/article/pii/S2213343723003743>
- [5] K. Bhardwaj, and A. K. Singh, "Bio-waste and natural resource mediated eco-friendly synthesis of zinc oxide nanoparticles and their photocatalytic application against dyes contaminated water," *Chemical Engineering Journal Advances*, vol. 16, Nov. 15, 2023. [Online]. Available: <https://www.sciencedirect.com/science/article/pii/S2666821123000935?via%3Dihub>
- [6] T. Dippong, E. A. Levei, and O. Cadar, "Recent advances in synthesis and applications of  $\text{MFe}_2\text{O}_4$  (M = Co, Cu, Mn, Ni, Zn) Nanoparticles," *Nanomaterials*, vol. 11, no. 6, Jun. 13, 2021. [Online]. Available: <https://pubmed.ncbi.nlm.nih.gov/34199310/>
- [7] I. Fatimah, I. Yanti, H. K. Wijayanti, G. D. Ramanda, S. Sagadevan, M. Tamyiz, and R. Doong, "One-pot synthesis of Fe O /NiFe O nanocomposite from iron rust waste as reusable catalyst for methyl violet oxidation," *Case Studies in Chemical and Environmental Engineering*, vol. 8, May 13, 2023. [Online]. Available: <https://www.sciencedirect.com/science/article/pii/S2666016423000749?via%3Dihub>
- [8] K. N. Gupta, Y. Ghafari, S. Kim, J. Bae, S. K. Kim, and Md. Saifuddin, "Photocatalytic degradation of organic pollutants over  $\text{MFe}_2\text{O}_4$  (M= Co, Ni, Cu, Zn) nanoparticles at neutral pH," *Scientific Reports*, vol. 10, Mar. 18, 2020, Art. no. 4942. [Online]. Available: <https://www.nature.com/articles/s41598-020-61930-2>
- [9] L. T. N. Hoa, N. V. N. An, V. H. T. My, P. T. T. Giang, L. K. Top, H. T. C. Nhan, P. B. Thang, T. T. T. Van, and L. V. Hieu, "Silver decorated on cobalt ferrite nanoparticles as a reusable multifunctional catalyst for water treatment applications in non-radiation conditions," *RSC Advances*, vol. 13, pp. 24554-24564, May 13, 2023. [Online]. Available: <https://pubs.rsc.org/en/content/articlehtml/2023/ra/d3ra02950f>
- [10] M. N. Hosny, I. Gomaa, G. M. Elmahgary, and A. M. Ibrahim, "ZnO doped C: Facile synthesis, characterization and photocatalytic degradation of dyes," *Scientific Reports*, vol. 13, Aug. 30, 2023, Art. no. 14173. [Online]. Available: <https://www.nature.com/articles/s41598-023-41106-4>
- [11] M. Jamshaid, M. H. Khan, A. M. Nazir, A. M. Wattoo, K. Shahzad, M. Malik, and A. Rehman, "A novel bentonite-cobalt doped bismuth ferrite nanoparticles with boosted visible light induced photodegradation of methyl orange: synthesis, characterization and analysis of physiochemical changes," *International Journal of Environmental Analytical Chemistry*, vol. 10, no. 5, p. 104, Dec. 19, 2024. [Online]. Available: <https://www.tandfonline.com/doi/full/10.1080/03067319.2022.2032014>
- [12] F. Kanwal, I. Rani, A. Batool, Y. Sandali, A. Li, A. Shafique, A. Irfan, and M. Sulaman, "Enhanced dielectric and photocatalytic properties of  $\text{TiO}_2$ -decorated rGO/PANI hybrid composites synthesized by in-situ chemical oxidation polymerization route," *Materials Science and Engineering*, vol. 298, Dec. 2023. [Online]. Available: <https://www.sciencedirect.com/science/article/pii/S0921510723005792?via%3Dihub>
- [13] C. Karthikeyan, P. Arunachalam, K. Ramachandran, M. A. Al-Mayouf, and S. Karuppuchamy, "Recent advances in semiconductor metal oxides with enhanced methods for solar photocatalytic applications," *Journal of Alloys and Compounds*, vol. 828, Jul. 05, 2020. [Online]. Available: <https://www.sciencedirect.com/science/article/pii/S09255838820306447?via%3Dihub>
- [14] G. N. Kokilaa, C. Mallikarjunaswamy, and V. Lakshmi Ranganatha, "A review on synthesis and applications of versatile nanomaterials," *Inorganic and Nano-Metal Chemistry*, vol. 54, Aug. 13, 2024. [Online]. Available: <https://www.tandfonline.com/doi/full/10.1080/24701556.2022.2081189>
- [15] A. P. Luque-Morales, A. López-Peraza, J. O. Nava-Olivas, G. Amaya-Parra, A. Y. Báez-López, V. M. Orozco-Carmona, H. E. Garrafa-Gálvez, and M.

- D. J. Chinchillas-Chinchillas, "ZnO semiconductor nanoparticles and their application in photocatalytic degradation of various organic dyes," *Materials*, vol. 14, no. 7537, p. 24, Dec. 08, 2023. [Online]. Available: <https://www.mdpi.com/1996-1944/14/24/7537>
- [16] P. Manimegalai, K. Selvam, S. Loganathan, D. Kirubakaran, M. S. Shivakumar, M. Govindasamy, U. Rajaji, and A. A. A. Bahajaj, "Green synthesis of zinc oxide (ZnO) nanoparticles using aqueous leaf extract of *Hardwickia binata*: Their characterizations and biological applications," *Biomass Conversion and Biorefinery*, vol. 14, no. 11, pp. 12559–12574, May 11, 2023. [Online]. Available: [file:///C:/Users/Sangeeta/Downloads/Green\\_synthesis\\_of\\_zinc\\_oxide\\_ZnO\\_nanoparticles\\_us.pdf](file:///C:/Users/Sangeeta/Downloads/Green_synthesis_of_zinc_oxide_ZnO_nanoparticles_us.pdf)
- [17] J. B. B. Mognol, F. Waanders, S. K. O. Ntwampe, E. Fosso-Kankeu, and A. R. A. Alilli, "Synthesis of eco-friendly ZnO-based heterophotocatalysts with enhanced properties under visible light in the degradation of organic pollutants," *Environmental Systems Research*, vol. 11, Nov. 20, 2022, Art. no. 25. [Online]. Available: <https://environmentalsystemsresearch.springeropen.com/articles/10.1186/s40068-022-00271-7>
- [18] H. M. Mousa, J. F. Alenezi, I. M. A. Mohamed, A. S. Y. Yasin, A. F. M. Hashem, and A. Abdal-Hay, "Synthesis of TiO<sub>2</sub>@ZnO heterojunction for dye photodegradation and wastewater treatment," *Journal of Alloys and Compounds*, vol. 886, Dec. 15, 2021. [Online]. Available: <https://www.sciencedirect.com/science/article/pii/S0925838821025780?via%3Dihub>
- [19] G. Nabi, A. Majid, A. Riaz, T. Alharbi, M. A. Kamran, and M. Al-Habardi, "Green synthesis of spherical TiO<sub>2</sub> nanoparticles using Citrus Limetta extract: Excellent photocatalytic water decontamination agent for RhB dye," *Inorganic Chemistry Communications*, vol. 129, Jul. 2021. [Online]. Available: <https://www.sciencedirect.com/science/article/pii/S1387700321001775?via%3Dihub>
- [20] H. A. L. D. Oliveira, G. Gomide, C. A. D. M. Vieira, A. A. A. M. Guerra, J. Depeyrot, and A. F. C. Campos, "Hybrid magnetic CoFe<sub>2</sub>O<sub>4</sub>@ $\gamma$ -Fe<sub>2</sub>O<sub>3</sub>@CTAB nanocomposites as efficient and reusable adsorbents for Remazol Brilliant Blue R dye," *Environmental Technology*, vol. 25, pp. 581–597, Oct. 21, 2022. [Online]. Available: <https://www.tandfonline.com/doi/full/10.1080/09593330.2022.2115946>
- [21] V. H. Rathi, A. R. Jiece, and K. Jayakumar, "Green synthesis of Ag/CuO and Ag/ TiO<sub>2</sub> nanoparticles for enhanced photocatalytic dye degradation, antibacterial, and antifungal properties," *Applied Surface Science Advances*, vol. 18, Dec.2023. [Online]. Available: <https://www.sciencedirect.com/science/article/pii/S2666523923001101?via%3Dihub>
- [22] S. Rajan, A. Venugopal, H. Kozhikkalathil, S. Valappil, M. Kale, M. Mann, P. Ahuja, and S. Munjal, "Synthesis of ZnO nanoparticles by precipitation method: Characterizations and applications in decipherment of latent fingerprints," *Materials Today Proceedings*, n.d. [Online]. Available: <https://www.sciencedirect.com/science/article/pii/S2214785323033151?via%3Dihub>
- [23] M. Rekaby, A. I. Abou-Aly, and M. El-Khatib, "Preparation and characterization of a novel nanocomposite based on MnCr-layered double oxide and CoFe<sub>2</sub>O<sub>4</sub> spinel ferrite for methyl orange adsorption," *Scientific Reports*, vol. 13, Oct. 21, 2023, Art. no. 18006. [Online]. Available: <https://www.nature.com/articles/s41598-023-45136-w>
- [24] F. Riyanti, N. Nurhidayah, W. Purwaningrum, N. Yuliasari, and P. L. Hariani, "MgFe<sub>2</sub>O<sub>4</sub> magnetic catalyst for photocatalytic degradation of Congo Red Dye in aqueous solution under visible light irradiation," *Environment and Natural Resources Journal*, vol. 21, no. 4, Jun. 23, 2023.
- [25] S. J. Salih, and W. M. Mahmood, "Review on magnetic spinel ferrite (MFe<sub>2</sub>O<sub>4</sub>) nanoparticles: From synthesis to application," *Heliyon*, vol. 9, no. 6, Jun. 2023. [Online]. Available: <https://www.sciencedirect.com/science/article/pii/S2405844023038082?via%3Dihub>
- [26] Y. Sun, W. Zhang, Q. Li, H. Liu, and X. Wang, "Preparations and applications of zinc oxide based photocatalytic materials," *Advanced Sensor and Energy Materials*, vol. 2, no. 3, Sept. 2023. [Online]. Available: <https://www.sciencedirect.com/science/article/pii/S2773045X23000249?via%3Dihub>
- [27] X. Shu, "Research on photoelectric properties of ZnO-based material," *Journal of Physics, Conference Series* 2541, 2023. [Online]. Available: <https://iopscience.iop.org/article/10.1088/1742-6596/2541/1/012060/pdf>
- [28] B. H. Taymaz, M. Demir, H. Kamaş, H. Orhan, Z. Aydoğan, and A. Akıllı, "Facile and green synthesis of ZnO nanoparticles for effective photocatalytic degradation of organic dyes and real textile wastewater," *International Journal of Phytoremediation*, vol. 25, no. 1–15, pp. 1306–1317, Nov. 28, 2022. [Online]. Available: <https://www.tandfonline.com/doi/full/10.1080/15226514.2022.2150142>
- [29] Q. Y. Tamboli, S. M. Patange, Y. K., Mohanta, R. Sharma, and K. R. Zakde, "Green synthesis of cobalt ferrite nanoparticles: An emerging material for

environmental and biomedical applications,” *Journal of Nanomaterials*, vol. 2023, no. 1, Feb. 6, 2023. [Online]. Available: <https://onlinelibrary.wiley.com/doi/10.1155/2023/9770212>

- [30] C. Vanitha, R. Abirami, S. Chandraleka, M. R. Kuppusamy, and T. M. Sridhar, “Green synthesis of

photocatalyst hydroxyapatite doped TiO<sub>2</sub>/GO ternary nanocomposites for removal of methylene blue dye,” *Materials Today: Proceedings*, Mar. 6, 2023. [Online]. Available: <https://www.sciencedirect.com/science/article/pii/S2214785323009203?via%3Dihub>